

# Synthesis, Structure, Band Gap, and Near-Infrared Photosensitivity of a New Chalcogenide Crystal, $(\text{NH}_4)_4\text{Ag}_{12}\text{Sn}_7\text{Se}_{22}$

Ke-Zhao Du,<sup>†</sup> Xing-Hui Qi,<sup>†,‡</sup> Mei-Ling Feng,<sup>†</sup> Jian-Rong Li,<sup>†</sup> Xing-Zhi Wang,<sup>§</sup> Cheng-Feng Du,<sup>†,||</sup> Guo-Dong Zou,<sup>†</sup> Meng Wang,<sup>†</sup> and Xiao-Ying Huang<sup>\*,†</sup>

<sup>†</sup>State Key Laboratory of Structural Chemistry, Fujian Institute of Research on the Structure of Matter, Chinese Academy of Sciences, Fuzhou, Fujian 350002, People's Republic of China

<sup>‡</sup>College of Chemistry and Chemical Engineering, Fuzhou University, Fuzhou, Fujian 350002, People's Republic of China

<sup>||</sup>University of Chinese Academy of Sciences, Beijing 100049, People's Republic of China

<sup>§</sup>Division of Physics and Applied Physics, School of Physical and Mathematical Sciences, Nanyang Technological University, Singapore 637371, Singapore

## Supporting Information

**ABSTRACT:** A new chalcogenide crystal,  $(\text{NH}_4)_4\text{Ag}_{12}\text{Sn}_7\text{Se}_{22}$  (FJSM-STs), has been solvothermally synthesized. The crystal structure, which is composed of arrays of  $[\text{Sn}_3\text{Se}_9]_n^{6n-}$  chains interconnecting  $[\text{SnAg}_6\text{Se}_{10}]_n^{10n-}$  and  $[\text{Ag}_3\text{Se}_4]_n^{5n-}$  layers, is unprecedented among the reported A/Ag/Sn/Q (A = cation; Q = S, Se, and Te) compounds. Optical absorption together with theoretical calculations of the band structure indicate a direct band gap of 1.21 eV for FJSM-STs, which is close to the ideal band gap to maximize the photoconversion efficiency proposed by Shockley and Queisser. The toxic-metal-free crystal of FJSM-STs exhibits obvious photosensitivity in the near-infrared range. The variates of power and temperature on the photosensitivity have been studied.

Since the discovery of infrared radiation in the early 19th century, several kinds of materials have been explored as infrared photodetectors, which have played an important role in the military and civil fields.<sup>1</sup> Among the infrared photodetection materials, metal chalcogenides with narrow band gap make up a large part.<sup>2</sup> However, reported chalcogenide materials such as PbS, HgCdTe, and PbSnTe usually contain toxic heavy metals, which limits their applications. Thus, the exploration of narrow-band-gap semiconducting chalcogenide crystals without a toxic-metal element would provide more candidates for infrared photodetection.

In addition, the new chalcogenide compounds have attracted much attention for their interesting physical and chemical properties, which may be found useful in other applications such as hard radiation detection, radioactive elements removal, etc.<sup>3</sup> Recently, one of the strategies of constructing novel chalcogenides is to introduce heterometal ions into one structure in which the two or three types of metal ions adopt a variety of coordination modes when bonded to chalcogen anions Q (Q = S, Se, and Te). For instance, monovalent  $\text{Ag}^+$  can coordinate to the chalcogen, forming linear, trigonal, to tetrahedral geometries, while  $\text{Sn}^{4+}$  can coordinate to four, five, or even six chalcogen ions;<sup>4</sup> such rich variation of the coordination modes may result in

A/Ag/Sn/Q (A = cation) compounds with structural diversity. Indeed, to date, a few kinds of Ag/Sn/Q anions have been reported, including 2D  $[\text{Ag}_2\text{Sn}_3\text{S}_9]_n^{4n-}$ ,<sup>5</sup> 3D  $[\text{Ag}_6\text{Sn}_3\text{S}_{10}]_n^{2n-}$ ,<sup>6</sup> 1D  $[\text{AgSn}_3\text{Se}_8]_n^{3n-}$ ,<sup>7</sup> 1D  $[\text{Ag}_2\text{Sn}_2\text{Se}_6]_n^{2n-}$ ,<sup>8</sup> 2D  $[\text{AgSn}_{12}\text{Se}_{28}]_n^{7n-}$ ,<sup>4a</sup> 3D  $[\text{Ag}_5\text{Sn}_4\text{Se}_{12}]_n^{3n-}$ ,<sup>4b</sup> 2D  $[\text{Ag}_6\text{Sn}_2\text{Te}_8]_n^{2n-}$  and 2D  $[\text{Ag}_2\text{SnQ}_4]_n^{2n-}$ ,<sup>4d,10</sup> where D refers to structural dimensionality. Most of these A/Ag/Sn/Q compounds are semiconductors with narrow band gap below 1.80 eV (Table S1). However, their infrared photoelectronic application has never been studied.

Herein we report on the synthesis, crystal structure, and characterizations of a novel Ag/Sn/Se compound,  $(\text{NH}_4)_4\text{Ag}_{12}\text{Sn}_7\text{Se}_{22}$  (FJSM-STs), which features a 3D anionic structure of  $[\text{Ag}_{12}\text{Sn}_7\text{Se}_{22}]_n^{4n-}$ . The optical band gap and near-infrared photosensitivity, as well as the theoretical band structure and density of states (DOS) of FJSM-STs, have been studied.

FJSM-STs was obtained from the solvothermal reaction described in the Supporting Information. Single-crystal X-ray crystallography revealed that FJSM-STs belongs to the space group  $C2/c$ . The asymmetric unit of FJSM-STs contains  $3^{-1/2}\text{Sn}^{4+}$ ,  $6\text{Ag}^+$ ,  $11\text{Se}^{2-}$ , and  $2\text{NH}_4^+$ ; the  $1/2\text{Sn}^{4+}$  is located in a 2-fold rotation axis. The coordination modes of these atoms are shown in Figure S2. Its structure features a 3D anionic framework with cages filled with  $\text{NH}_4$  cations as charge-balancing agents, forming intensive N–H...Se hydrogen bonds with the anionic framework (Figure S3 and Table S2). The solvent-accessible volume excluding the ammonium cations in FJSM-STs is  $\sim 9.0\%$  calculated by PLATON.<sup>11</sup>

Overall, the anionic 3D  $[\text{Ag}_{12}\text{Sn}_7\text{Se}_{22}]_n^{4n-}$  framework is constructed of arrays of  $[\text{Sn}_3\text{Se}_9]_n^{6n-}$  chains interconnecting  $[\text{SnAg}_6\text{Se}_{10}]_n^{10n-}$  by sharing Se3, Se4, and Se6 and  $[\text{Ag}_3\text{Se}_4]_n^{5n-}$  layers by sharing Se7, Se9, Se10, and Se11 (Figure 1a). As illustrated in Figures 1b and S4,  $[\text{SnAg}_6\text{Se}_{10}]_n^{10n-}$  exhibits a trilayer structure extended along the  $bc$  plane. The  $\text{Ag}_1\text{Se}_4$  and  $\text{Ag}_3\text{Se}_4$  tetrahedra are interconnected to form a  $(6^3)[\text{Ag}_2\text{Se}_5]_n^{8n-}$  layer by core-sharing of the Se1, Se2, and Se3 atoms, and then two such  $[\text{Ag}_2\text{Se}_5]_n^{8n-}$  layers are alternately interconnected by a pair of  $[\text{Ag}_2\text{Se}_3]$  by corner-sharing of the Se1, Se2, and Se3

Received: March 31, 2016

Published: May 26, 2016

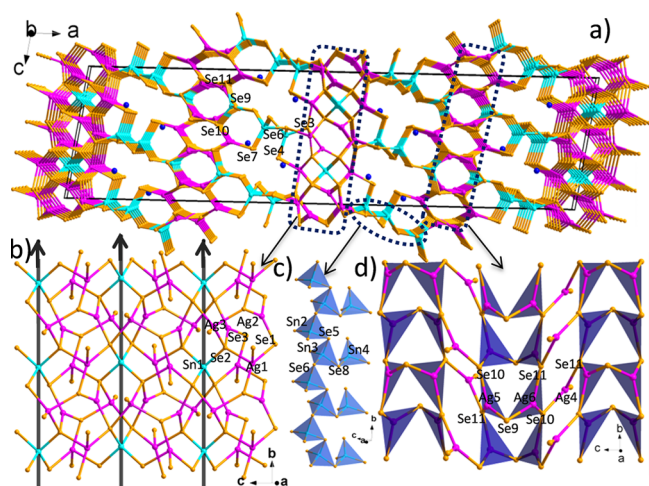


**Figure 1.** (a) 3D FJSM-STs structure viewed along the  $b$  axis. H atoms are omitted for clarity. (b)  $[\text{SnAg}_6\text{Se}_{10}]_n^{10n-}$  layer. The arrows represent the 2-fold rotation axes. (c)  $[\text{Sn}_3\text{Se}_9]_n^{6n-}$  chain. (d)  $[\text{Ag}_3\text{Se}_4]_n^{5n-}$  layer.

atoms and  $[\text{Sn}1\text{Se}_4]$  by corner-sharing of the Se1 and Se2 atoms to form the sandwich-like  $[\text{SnAg}_6\text{Se}_{10}]_n^{10n-}$  layer, in which the 2-fold rotation axes passing through the Sn1 atoms are parallel to the  $b$  axis. Figure 1c shows a  $[\text{Sn}_3\text{Se}_9]_n^{6n-}$  chain extended along the  $b$  axis, which is formed by  $[\text{Sn}3\text{Se}_4]$  connecting  $[\text{Sn}2\text{Se}_4]$  and  $[\text{Sn}4\text{Se}_4]$  via corner-sharing of the Se5, Se6, and Se8 atoms. As shown in Figure 1d, the planar-trigonal  $[\text{Ag}5\text{Se}_3]$  and  $[\text{Ag}6\text{Se}_3]$  corner-share the Se9, Se10, and Se11 atoms to form a  $[\text{Ag}_2\text{Se}_3]_n^{4n-}$  ribbon; the ribbons are further interconnected into a  $[\text{Ag}_3\text{Se}_4]_n^{5n-}$  layer by  $[\text{Ag}4\text{Se}_3]$  through corner-sharing of the Se10 and Se11 atoms with Ag6 and Ag5, respectively.

The anionic framework of FJSM-STs is unprecedented and much more complex than those of the previously reported A/Ag/Sn/Se compounds, which normally are constructed from two simple structural units, as described below and illustrated in Figure S5. For instance, the  $[\text{AgSn}_{12}\text{Se}_{28}]_n^{7n-}$  layer is formed by Ag atoms with linear coordination geometry interconnecting  $[\text{Sn}_{12}\text{Se}_{28}]_n^{8n-}$  double chains (Figure S5a),<sup>4a</sup> while the 3D  $[\text{Ag}_5\text{Sn}_4\text{Se}_{12}]_n^{3n-}$  framework is composed by  $[\text{Sn}_2\text{Se}_6]$  units interlinking  $[\text{Ag}_5\text{Se}_8]_n^{11n-}$  chains (Figure S5b).<sup>4b</sup> The regular  $[\text{AgSn}_3\text{Se}_8]_n^{3n-}$  chain is composed of an alternating arrangement of edge-sharing  $[\text{Sn}_3\text{Se}_8]$  and  $[\text{AgSe}_4]$  units (Figure S5c),<sup>7a</sup> whereas the  $[\text{Ag}_2\text{Sn}_2\text{Se}_6]_n^{2n-}$  chain is formed through two  $[\text{AgSe}_2]$  units interconnecting  $[\text{Sn}_2\text{Se}_6]$  units (Figure S5d).<sup>8</sup> The last example is the  $[\text{Ag}_2\text{SnSe}_4]_n^{2n-}$  layer, which is constructed by  $[\text{SnSe}_4]$  units interconnecting two  $[\text{AgSe}_2]_n^{3n-}$  chains by edge-sharing of  $\mu_3\text{-Se}$  (Figure S5e).<sup>10b</sup>

The optical absorption spectrum of the title compound, which is converted from solid diffuse reflectance using the Tauc equation, indicates a band gap of around 1.21 eV for FJSM-STs.<sup>12</sup> The narrow band gap is consistent with the black color of the crystals (Figure 2a). Compared with that of the previously reported A/Ag/Sn/Se compounds such as  $[(\text{Me})_2\text{NH}_2]_{0.75}[\text{Ag}_{1.25}\text{SnSe}_3]$  (1.85 eV; Table S1), the band gap of FJSM-STs has a noticeable red shift.<sup>4b</sup> The higher density of the title compound (5.270 g/cm<sup>3</sup>) than that of  $[(\text{Me})_2\text{NH}_2]_{0.75}[\text{Ag}_{1.25}\text{SnSe}_3]$  (3.784 g/cm<sup>3</sup>) might cause the absorption of visible light, which leads to the red shift. The DOS calculations, together with the band structures, have been studied. The methodology is described in the Supporting Information. The calculated band gap of around 0.4 eV is direct, which is smaller than the experimental value (1.21 eV) (Figure

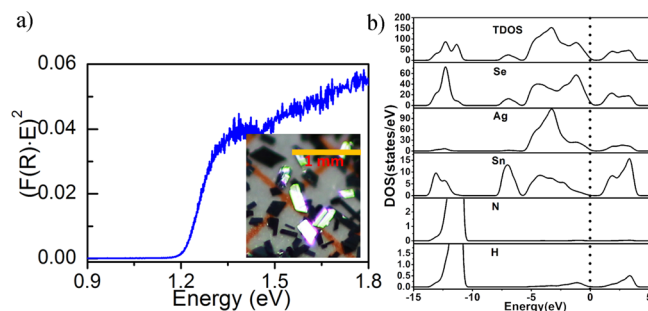


**Figure 2.** (a) Solid-state optical absorption spectrum of FJSM-STs. The inset is a photograph of the crystals. (b) Total and partial DOS of FJSM-STs. The Fermi level is set at 0 eV. The DOS curves are the sum of states of the electron orbitals.

S6). The lack of fidelity between the generalized gradient approximation and eigenvalues of the electronic states should be the reason for this quantitative underestimation.<sup>13</sup> As shown in the DOS curve of FJSM-STs (Figure 2b), the minimum of the conduction band above the Fermi level (the Fermi level is set at 0.0 eV) is mainly contributed by  $\text{Se}^{2-}$ ,  $\text{Ag}^+$ , and  $\text{Sn}^{4+}$ , while the maximum of the valence band is derived from  $\text{Se}^{2-}$  and  $\text{Ag}^+$ .  $\text{NH}_4^+$  contributes little to the band in this case. The direct band gap is around 1.21 eV, falling in the range from 1.0 to 1.8 eV, which was the most suitable band-gap range for the solar cell proposed by Shockley and Queisser.<sup>14</sup>

The narrow band gap of FJSM-STs suggests the near-infrared photoelectronic application. Power- and temperature-dependent photoelectronic experiments under a 980 nm laser have been carried out on a sensor substrate in a modified CGS-1TP intelligent sensing analysis system. The device preparation and measurement system can be found in Figure S7. FJSM-STs exhibits obvious near-infrared photosensitivity (Figure 3a). Photoconduction can be calculated from eq 1

$$g_p = g_l - g_d \quad (1)$$

where  $g_p$ ,  $g_l$ , and  $g_d$  are photoconduction, light conduction, and dark conduction, respectively.<sup>15</sup> From Figure 3a, we could see

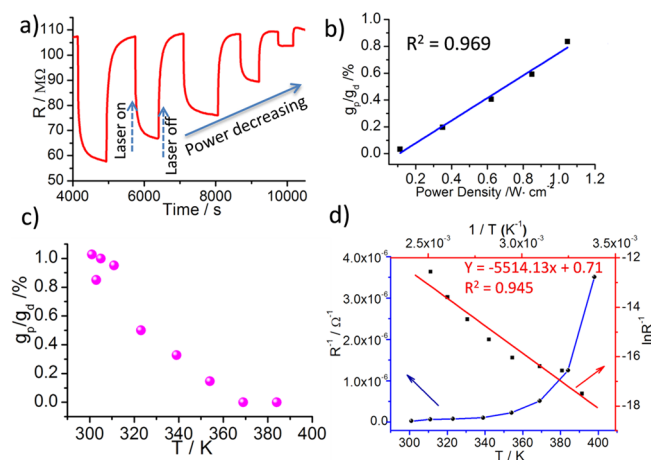


**Figure 3.** (a) Transient photoelectronic response of FJSM-STs versus time under a 980 nm laser with controllable power at room temperature. (b) Light-power-dependent  $g_p/g_d$  at room temperature. (c) Temperature-dependent  $g_p/g_d$  under a light power of 1.0 W/cm<sup>2</sup>. (d) Temperature-dependent dark conduction of the sample (blue curve). The red curve is fitted by the Arrhenius equation.  $g_p$  and  $g_d$  are photoconduction and dark conduction, respectively.

that every photoelectronic response under different laser power almost started from the same dark-conduction baseline ( $g_d$ ).  $g_i$  varied with different light power and temperature. Figure 3b was plotted from the data of Figure 3a.  $g_p/g_d$  increased near linearly as the laser power was increased (Figure 3b), which suggests one-photon absorption of 980 nm in the title material under 1.0 W/cm<sup>2</sup>. One-photon absorption is a linear absorption process, whereby simultaneous absorption of one photon excites the electron from one state (usually the ground state) to a higher energy electronic state. Higher temperature would induce a higher density of the thermal activated carrier, which could compete with the photoactivated carrier induced by laser irradiation. As shown in Figure 3c, the optical sensitivity decreased as the temperature was increased, and there is a thermal quenching around 370 K under 1.0 W/cm<sup>2</sup>, which is due to a photoactivated carrier suppressed by the thermally activated one.<sup>16</sup> The temperature-dependent resistance on polycrystalline FJSM-STs has been plotted in Figure 3d. As a semiconductor, the temperature-dependent conductivity of FJSM-STs can be fitted via the Arrhenius equation (2)

$$\sigma = C e^{-E/\kappa T} \quad (2)$$

where  $\sigma$  is the conductivity,  $C$  is a constant,  $\kappa$  is the Boltzmann constant, and  $E$  is an activation energy for electron conduction. From the fitting curve, the calculated activation energy is about 0.48 eV, which is smaller than the semiconductor (bdaH)InSe<sub>2</sub> (0.81 eV).<sup>17</sup>

In summary, we have presented the solvothermal synthesis, crystal structure, optical absorption, and photosensitivity behavior as well as theoretical band-gap calculations of a new chalcogenide crystal, FJSM-STs. The title compound, which was toxic-metal-free, exhibited an obvious photosensitivity in the near-infrared range. The solid-state optical absorption spectrum and band-structure calculations indicate a direct band gap of 1.21 eV of the title crystal, which is close to the ideal band gap to maximize the photoconversion efficiency proposed by Shockley and Queisser.

## ■ ASSOCIATED CONTENT

### Supporting Information

The Supporting Information is available free of charge on the ACS Publications website at DOI: 10.1021/acs.inorgchem.6b00803.

More experimental and calculated details, PXRD, more structural information, structural comparison with those of other A/Ag/Sn/Q compounds, and diagrams for calculated band structures (PDF)  
CCDC 1456475 for FJSM-STs (CIF)

## ■ AUTHOR INFORMATION

### Corresponding Author

\*E-mail: xyhuang@fjirms.ac.cn.

### Notes

The authors declare no competing financial interest.

## ■ ACKNOWLEDGMENTS

This work was supported by grants from the NNSF of China (Grants 21521061, 21371001, and 21373223), the 973 Program (Grant 2014CB845603), and the Chunmiao Project of the Haixi Institute of Chinese Academy of Sciences (Grant CMZX-2014-001).

## ■ REFERENCES

- (1) Saran, R.; Curry, R. J. *Nat. Photonics* **2016**, *10*, 81–92.
- (2) (a) Downs, C.; Vandervelde, T. E. *Sensors* **2013**, *13*, 5054–5098. (b) Rogalski, A. *Infrared Phys. Technol.* **2011**, *54*, 136–154. (c) Rogalski, A. *Prog. Quantum Electron.* **2003**, *27*, 59–210. (d) Rogalski, A. *Infrared Phys. Technol.* **2002**, *43*, 187–210.
- (3) (a) Wibowo, A. C.; Malliakas, C. D.; Liu, Z.; Peters, J. A.; Sebastian, M.; Chung, D. Y.; Wessels, B. W.; Kanatzidis, M. G. *Inorg. Chem.* **2013**, *52*, 7045–7050. (b) Johnsen, S.; Liu, Z.; Peters, J. A.; Song, J. H.; Nguyen, S.; Malliakas, C. D.; Jin, H.; Freeman, A. J.; Wessels, B. W.; Kanatzidis, M. G. *J. Am. Chem. Soc.* **2011**, *133*, 10030–10033. (c) Ding, N.; Kanatzidis, M. G. *Nat. Chem.* **2010**, *2*, 187–191. (d) Feng, M. L.; Kong, D. N.; Xie, Z. L.; Huang, X. Y. *Angew. Chem., Int. Ed.* **2008**, *47*, 8623–8626. (e) Qi, X. H.; Du, K. Z.; Feng, M. L.; Li, J. R.; Du, C. F.; Zhang, B.; Huang, X. Y. *J. Mater. Chem. A* **2015**, *3*, 5665–5673.
- (4) (a) Li, J. R.; Xiong, W. W.; Xie, Z. L.; Du, C. F.; Zou, G. D.; Huang, X. Y. *Chem. Commun.* **2013**, *49*, 181–183. (b) Li, J. R.; Huang, X. Y. *Dalton Trans.* **2011**, *40*, 4387–4390. (c) Dehnen, S.; Melullis, M. *Coord. Chem. Rev.* **2007**, *251*, 1259–1280. (d) An, Y. L.; Menghe, B.; Ye, L.; Ji, M.; Liu, X.; Ning, G. L. *Inorg. Chem. Commun.* **2005**, *8*, 301–303. (e) Sheldrick, W. S.; Wachhold, M. *Coord. Chem. Rev.* **1998**, *176*, 211–322. (f) Sheldrick, W. S.; Wachhold, M. *Angew. Chem., Int. Ed. Engl.* **1997**, *36*, 206–224. (g) Wood, P. T.; Pennington, W. T.; Kolis, J. W. *J. Chem. Soc., Chem. Commun.* **1993**, 235–236.
- (5) (a) BaiYin, M. H.; Ji, M.; Liu, X.; An, Y. L.; Jia, C. Y.; Ning, G. L. *Chem. J. Chinese Univ.* **2004**, *25*, 1391–1394. (b) An, Y. L.; Ji, M.; Baiyin, M.; Liu, X.; Jia, C. Y.; Wang, D. H. *Inorg. Chem.* **2003**, *42*, 4248–4249.
- (6) (a) BaiYin, M. H.; Ye, L.; An, Y. L.; Liu, X.; Jia, C. Y.; Ning, G. L. *Bull. Chem. Soc. Jpn.* **2005**, *78*, 1283–1284. (b) Baiyin, M.; An, Y. L.; Liu, X.; Ji, M.; Jia, C. Y.; Ning, G. L. *Inorg. Chem.* **2004**, *43*, 3764–3765.
- (7) (a) Ji, M.; Baiyin, M. H.; Ji, S. H.; An, Y. L. *Inorg. Chem. Commun.* **2007**, *10*, 555–557. (b) Yao, H. G.; Zhang, R. C.; Ji, S. H.; Ji, M.; An, Y. L.; Ning, G. L. *Inorg. Chem. Commun.* **2010**, *13*, 1296–1298.
- (8) Guo, H. Y.; Li, Z. H.; Yang, L.; Wang, P.; Huang, X. Y.; Li, J. *Acta Crystallogr., Sect. C: Cryst. Struct. Commun.* **2001**, *57*, 1237–1238.
- (9) Chen, Z.; Wang, R. J.; Li, J. *Chem. Mater.* **2000**, *12*, 762–766.
- (10) (a) Pienack, N.; Bensch, W. Z. *Anorg. Allg. Chem.* **2006**, *632*, 1733–1736. (b) Chen, X.; Huang, X. Y.; Fu, A. H.; Li, J.; Zhang, L. D.; Guo, H. Y. *Chem. Mater.* **2000**, *12*, 2385–2391.
- (11) Spek, A. *Acta Crystallogr., Sect. D: Biol. Crystallogr.* **2009**, *65*, 148–155.
- (12) (a) Tauc, J.; Grigorovici, R.; Vancu, A. *Phys. Status Solidi B* **1966**, *15*, 627–637. (b) Sasca, V.; Popa, A. *J. Appl. Phys.* **2013**, *114*, 133503.
- (13) (a) Du, K. Z.; Feng, M. L.; Li, L. H.; Hu, B.; Ma, Z. J.; Wang, P.; Li, J. R.; Wang, Y. L.; Zou, G. D.; Huang, X. Y. *Inorg. Chem.* **2012**, *51*, 3926–3928. (b) Du, K. Z.; Feng, M. L.; Qi, X. H.; Ma, Z. J.; Li, L. H.; Li, J. R.; Du, C. F.; Zou, G. D.; Huang, X. Y. *Dalton Trans.* **2014**, *43*, 2733–2736.
- (14) (a) Shockley, W.; Queisser, H. J. *J. Appl. Phys.* **1961**, *32*, 510–519. (b) Mathers, C. *J. Appl. Phys.* **1977**, *48*, 3181–3182.
- (15) Ceng, G.; Zhang, Z.; Zhang, C. *Optical Detection Technology*; Tsinghua University Press: Beijing, China, 2005.
- (16) Bube, R. H. *Photoelectronic properties of semiconductors*; Cambridge University Press: Cambridge, U.K., 1992.
- (17) Du, K. Z.; Hu, W. B.; Hu, B.; Guan, X. F.; Huang, X. Y. *Mater. Res. Bull.* **2011**, *46*, 1969–1974.